Lasers in Manufacturing Conference 2015

Influence of Welding Parameters and Stack Configuration on Pore Formation of Laser Welded Aluminum Foil Stacks

Thomas Engelhardt[a]*, Michael Brandner[a], Rudolf Weber[b], Thomas Graf[b]

[a]*Daimler AG, Mercedesstr. 137, 70327 Stuttgart, Germany*
[b]*Institut für Strahlwerkzeuge (IFSW), University of Stuttgart, Pfaffenwaldring 43, 70569 Stuttgart, Germany*

Abstract

Ultra-thin copper and aluminum foils with a thickness of 10 µm and 20 µm respectively are used as base material for the active layers in lithium ion batteries. In a pouch cell design, several layers of coated copper (anode) and aluminum (cathode) electrode foils are stacked alternately. All layers are separated by an ion conductive synthetic material. The uncoated aluminum foil contact tabs of all cathode layers must be welded in a stack configuration to an aluminum terminal sheet. On the anode side, the copper foil stack has to be welded to a copper terminal sheet.

Continuous wave laser welding of such aluminum foil stacks with up to 30 layers with a 1 µm wavelength fiber laser was investigated as presented in the following. Advantages in comparison to state of the art ultrasonic welds can be found in less mechanical stress from the joining process. However, especially this cathode laser weld shows imperfections such as porosity and sporadic separations of foils from the weld seam.

Seam porosity was characterized by computer tomography and image analysis of cross sections to investigate the influence of the welding parameters and the number of welded foils in the stack. It was noticed that the variation of these parameters affects the pore volume and distribution.

Aluminum Laser Welding, Ultra-Thin Foils, Foil Stack, Lithium-Ion Battery, Pore Formation

* Corresponding author. Tel.: +49 711 17 20579
E-mail address: thomas.t.engelhardt@daimler.com.

1. Introduction

Thin copper and aluminum foils are typically applied as base material for active layers in lithium ion accumulators [Yoshio, 2009]. An important process step in cell production is to join the electrode foil stack of contact tabs to a terminal sheet. The uncoated copper foils in a stack configuration are welded to a copper terminal sheet. On the cathode side, the aluminum foil stack is welded to an aluminum terminal sheet. Currently, the favored welding process is ultrasonic welding [Thiele, 2012]. This process can cause cracks in the foil layers because of high stress [Schedewy, 2011]. Investigations show that it is possible to join copper or aluminum foil stacks of 30 layers without a detrimental influence of stress in overlap configuration by continuous wave laser welding [Schedewy, 2011]. However, especially the weld seam of the aluminum cathode shows defects in terms of porosity and voids. This reduces the electric conductive cross section which may increase the contact resistance.

Various defect mechanisms in laser welding of aluminum which can affect seam porosity have already been discussed in literature. The investigation on bead on plate welding shows instabilities of the capillary bottom resulting in pore formation [Hohenberger, 2002][Rapp, 1996]. A further cause for pores can be the reduction of the solubility of hydrogen during the solidification of aluminum [Thier, 1976]. An additional reason for seam porosity in the weld configuration of foil stacks is supposed to be related to the great number of layers and surfaces. On the one hand, the aluminum foil surface usually consists of an Al_2O_3 layer [Ostermann, 2007]. On the other hand, air remains trapped between the foils also in the melting zone due to the surface topology and the gaps between the foils. Hence, it is assumed that seam porosity also depends on the number of foils in the stack.

The continuous-wave laser welding experiments described in the following were carried out to investigate the influence of the number of foils and the feed rate on pore formation. The examinations in this paper should support understanding of pore formation during laser welding of aluminum foil stacks and show possibilities to minimize the pore volume.

2. Experiments

The pore size and distribution were determined in stacks welded with feed rates of 10 m/min and 30 m/min. A 5 kW fiber laser (λ = 1070 nm) with a scan head was used, the resulting spot size was d_f = 100 µm. Uncoated Al 99.5 foils with a thickness of 20 µm and Al 99.5 terminal sheets with a thickness of 0.5 mm were used and welded in overlap configuration as shown in figure 1 with a seam length l of 30 mm. The specimens were clamped by an electromagnetic clamping device which generates a pressure of 1.6 N/mm². An additional Al 99.5 clamping sheet with a thickness s = 0.5 mm was used. Different numbers of foil layers N_L, varying between 5 and 30, were examined. The foils were cleaned and dried before the stack preparation. The laser power was adapted to the two feed rates and the foil layer amount to get approximately the same weld depth of about 0.4 mm in the terminal sheet. Figure 1 shows the weld configuration of an aluminum foil stack and the experimental setup.

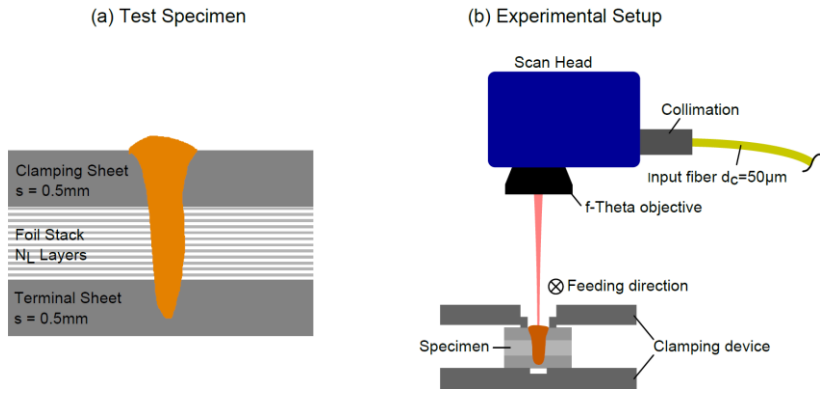

Fig. 1. (a) Weld configuration of an aluminum stack with N_L layers of Al99.5 foils (thickness 20 µm), aligned between an Al99.5 terminal sheet and a clamping sheet (s = 0.5mm) in a sandwich configuration; (b) Experimental setup.

2.1. Determination of Porosity

Computer tomographic analysis (CT) of weld seams was used for 3D pore detection. Furthermore, longitudinal (LCS) and transversal (TCS) 2D cross sections were prepared from the specimen by metallographic analysis. The pore size and amount was determined by measuring the area of each pore $A_{P,i}$ from the 2D cross sections. It can be used to approximate seam porosity [Allen, 1996]. The amount of pore area was related to the molten area A_M. Hence, the ratio of weld seam porosity from a 2D cross section is

$$x_P = \frac{\sum_{i=1}^{k} A_{P,i}}{A_M}. \qquad (1)$$

The pore size and distribution was determined by image analysis. Figure 2 shows the measured quantities and the steps of image processing applied on a longitudinal cross section of a foil stack weld.

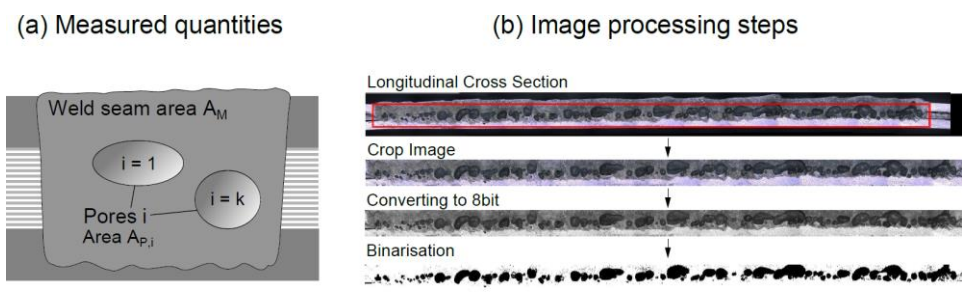

Fig. 2. (a) Sketch of a longitudinal cross section with the measured quantities of the weld seam area A_M and the areas of k pores $A_{P,i}$; (b) Image processing steps of a longitudinal cross section for pore size determination (P = 1 kW, v = 10 m/min, N_L = 15). The pore ratio x_P is calculated from the binary picture.

The seam area within the solid material was considered. An ImageJ particle analysis recognized connected pixel areas. Thus, the pore sizes $A_{P,i}$ were measured from binary picture which is considered for the calculation of x_P.

2.2. Results

The results of a CT analysis from weld seams at 10 m/min and 30 m/min with 30 foil layers are shown in figure 3. Huge pores occur along the whole seam length at 10m/min which are mainly located in the foil stack region. The pore size and distribution differs between welding speeds. A higher amount of small pores at 30 m/min exist in the weld seam in comparison to 10 m/min.

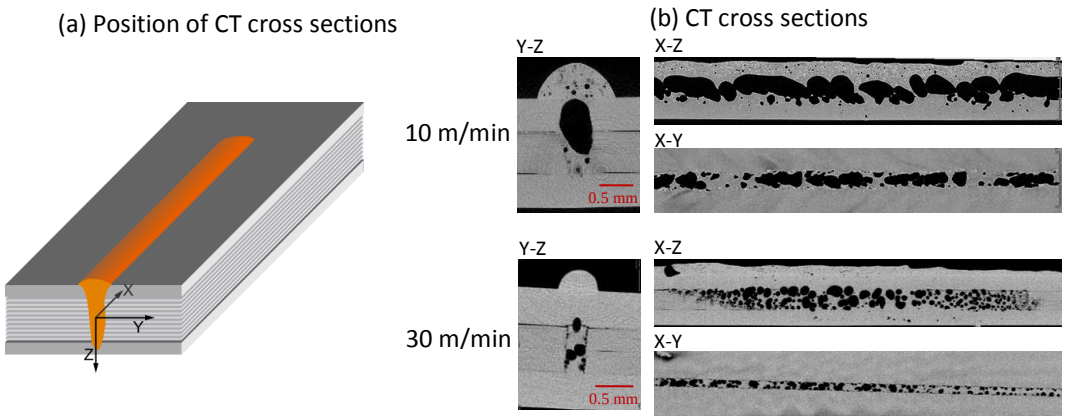

Fig. 3. (a) Sketch of a foil stack weld with the origin of ordinates; (b) CT-Analysis of laser welded aluminum foil stacks (30 Layers) at a feed rate of 10 m/min (top) and 30 m/min (bottom). The Y-Z plane corresponds to a transversal cross section, X-Z corresponds to a longitudinal cross section.

The pore ratio x_P which is dependent on the number of foil layers N_L at feed rates of 10 m/min and 30m/min is shown in figure 4. x_P increases approximately with an increase of the foil layer amount. This was observed in the longitudinal and transversal cross section. A decrease of the feed rate to 10 m/min results in an increase of the pore volume, which may be due to a longer time where the gas bubbles can expand in the melt pools.

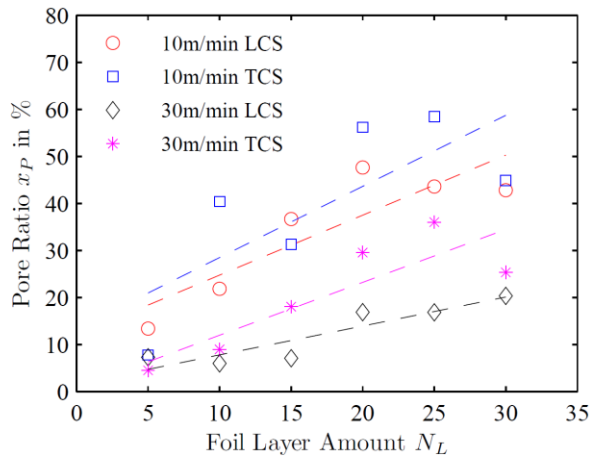

Fig. 4. Pore ratio x_P from the metallographic analysis of longitudinal (LCS) and transversal (TCS) cross sections, depending on the foil layer amount N_L at feed rates of 10 m/min and 30 m/min. The dashed trend lines are linear fits of the data points.

The histograms in figure 5 show the distribution of the measured pore areas $A_{P,i}$ in relation to the feed rate and the number of foils. At 10 m/min with 30 layers (Fig. 5(a)), large elongated pores occur in the weld seam with a pore size area of > 5 mm². Increasing the feed rate up to 30 m/min results in more counts of pores at $A_{P,i}$ < 0.1 mm². Huge elongated pores of $A_{P,i}$ > 5 mm² are suppressed. A variation of the foil layer amount at a fixed welding speed of 10 m/min (Fig. 5(b)) shows more than 100 small ($A_{P,I}$ < 0.1 mm²) and also large pores ($A_{P,I}$ > 1 mm²) at N_L = 30 in comparison to the case with 5 layers. A small amount of pores with $A_{P,i}$ < 0.1 mm² was detected in the weld seam joining 5 foil layers. Hence, a minimal pore ratio of ≈ 5% and small pores was reached at high feed rate and small foil layer amount.

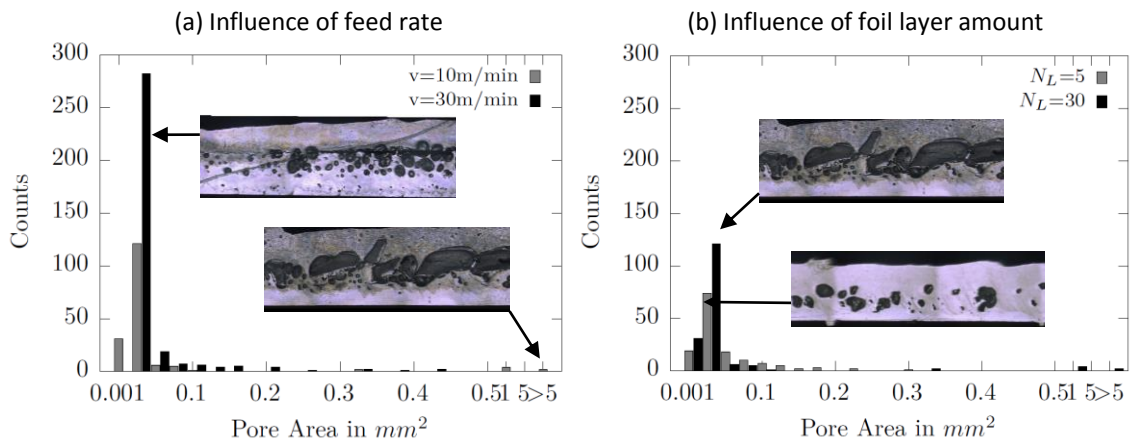

Fig. 5. (a) Pore size distribution at different feed rates v (N_L = 30) with the number of counts at determined pore areas $A_{P,i}$; (b) Pore size distribution for different number of foil layers N_L at a feed rate of 10m/min; The longitudinal cross sections show the seam porosity of the corresponding weld parameter and stack configuration.

2.3. Discussion

A surface analysis of aluminum foils shows a rough texture from the cold rolling process. The determined roughness average R_a is 0.12 µm. In consideration of an ideal clamp, ambient atmosphere can remain between the foil layers. It is supposed that this volume contributes to the resulting seam porosity. A first estimation of the amount of gas enclosed in the pores indicates that it correlates well with the volume of air enclosed between the foils in the area covered by the weld seam.

The decrease of the solubility of hydrogen around 20 times from the liquid to solid phase is a major reason for pore formation in aluminum materials [Ostermann, 2007]. Molecular hydrogen leads to seam porosity by precipitation from the aluminum melt during the solidification. Sources of hydrogen are atmospheric humidity, enclosed parts in the oxide layers and surface contamination [Altenpohl, 1965][Dilthey, 2005]. It is assumed that the significance of pores from hydrogen increases with an increase of the number of foils in the stack and gaps between foil layers. The influence of the great number of Al_2O_3 aluminum oxide layers on the foil surfaces in the area covered by the weld seam has to be clarified as well. A more detailed discussion of the supposed seam defects will be reported within further investigations.

3. Conclusion

Continuous wave laser welding of aluminum foil stacks from 5 to 30 layers with a 1 µm wavelength fiber laser was investigated for the present paper. The resulting seam porosity was analyzed by an image analysis of longitudinal and transversal seam cross sections. It was measured that pore ratio x_P of the weld seam increases with an increase of the foil layer amount. The size and distribution can be influenced by the feed rate whereas a greater amount of small pores occur at 30 m/min in comparison to 10 m/min. A seam pore ratio of ≈ 5% was observed with the configuration of 5 layers at 30 m/min. The reason for the observed porosity is supposed in air gaps between foil layers, an increased amount of available hydrogen sources and oxide layers. Further investigations may clarify the influence of gaps by eliminating the ambient atmosphere between foil layers completely.

References

Yoshio, M., R. J. Brodd und A. Kozawa: Lithium-Ion Batteries. Springer Science+Business Media, New York, 2009.

Thiele, R., U. Reisgen und M. Schleser: Schweißverbindungen in Lithium-Ionen- Batterien. In: DVS Congress 2012 , Bd. 286, S. 157-161.

Schedewy, R., E. Beyer, B. Brenner und J. Standfuss: Prospects of welding Foils with Solid State Laser for Lithium-Ion Batteries. In: ICALEO 2011 , Bd. 2011.

Hohenberger, B.: Laserstrahlschweißen mit Nd:YAG-Doppelfokustechnik - Steigerung von Prozessstabilität, Flexibilität und verfügbarer Strahlleistung. Doktorarbeit, Universität Stuttgart, Stuttgart, 2002.

Rapp, J.: Laserschweißeignung von Aluminiumwerkstoffen für Anwendungen im Leichtbau. Doktorarbeit, Universität Stuttgart, Stuttgart, 1996.

Thier, H.: Ursachen der Porenbildung beim Schutzgasschweißen von Aluminium und Aluminiumlegierungen. Schweißen und Schneiden, 1973(25):5.491–494, 1973.

Ostermann, F. und W. Thieler: Anwendungstechnologie Aluminium: Ein werkstoffhandbuch. Springer-Verlag, Berlin and Heidelberg, 3. Auflage, 2007.

Allen, T. (Hrsg.): Particle Size Measurement. Volume 1: Surface Area and Pore Size Determination, Volume 2: Powder Sampling and Particle Size Measurement. Springer Verlag, Dordrecht, 1996.

Altenpohl, D.: Aluminium und Aluminiumlegierungen. Springer-Verlag, Berlin and Heidelberg, 1965.

Dilthey, U.: Schweißtechnische Fertigungsverfahren 2: Verhalten der Werkstoffe beim Schweißen. Springer-Verlag, Berlin and Heidelberg, 3. Auflage, 2007.